ELSEVIER

Nuclear Physics A 613 (1997) 147–164

NUCLEAR PHYSICS A

Higher-order effects in the Coulomb dissociation of ^{8}B into ^{7}Be + p

S. Typel [a,1], H.H. Wolter [a], G. Baur [b]

[a] *Sektion Physik, Universität München, Am Coulombwall 1, D-85748 Garching, Germany*

[b] *Institut für Kernphysik, Forschungszentrum Jülich, D-52425 Jülich, Germany*

Received 17 September 1996; revised 14 October 1996

Abstract

Corrections to the first-order semiclassical description of the electromagnetic breakup of ^{8}B in heavy-ion collisions are studied. Second- and third-order corrections to the Coulomb dissociation of light projectiles in heavy-ion collisions are calculated in an approximation for small adiabaticity parameters. Quantum mechanical diffraction effects are investigated in a simple approximation obtained from Glauber theory. The methods are applied to the ^{8}B breakup at projectile energies of 46.5 and 250 A·MeV. Implications on the extraction of the astrophysical S-factor of the inverse ^{7}Be(p,γ)^{8}B reaction, which is relevant to the solar neutrino problem, are discussed.

PACS: 25.70.Mn; 25.70.De; 25.40.Lw; 27.20.+n

Keywords: Coulomb dissociation, Higher-order effects, Diffraction effects, ^{7}Be(p,γ)^{8}B astrophysical S-factor

1. Introduction

The electromagnetic dissociation of ^{8}B in fast peripheral heavy-ion collisions has recently been used as an indirect method to obtain information about the ^{7}Be(p,γ)^{8}B reaction. At low energies the cross section of this radiative capture reaction determines the flux of high-energy neutrinos through the subsequent β^+ decay of ^{8}B. Therefore, it is of particular interest in the high-energy solar neutrino problem [1,2]. The difficulties of a direct measurement of the capture reaction are discussed in Ref. [3]. Therefore, the indirect Coulomb dissociation method may help to independently determine the cross section. The breakup of ^{8}B may also provide valuable information about the existence

[1] E-mail: stypel@laser.physik.uni-muenchen.de.

PII S0375-9474(96)00415-0

of a proton halo in the ^{8}B ground state, e.g. by studying the momentum distributions of the fragments [4,5].

The breakup of ^{8}B in heavy-ion collisions has already been studied in various experiments. Momentum distribution and total breakup cross sections were investigated with respect to the halo structure over a large range of energies on light and heavy targets [5–7]. The objective of an experiment at RIKEN [8] with a projectile energy of 46.5 A·MeV on a Pb target was the determination of the S-factor of the ^{7}Be(p,γ)^{8}B reaction. In subsequent experiments the accuracy of this result was improved and it was tried to gain additional information about different multipole contributions to the breakup [9,10]. An experiment at NSCL/MSU is currently being evaluated [11]. A further experiment for the determination of the astrophysical S-factor is planned at GSI with a much higher ^{8}B energy of 250 A·MeV.

There are several assumptions which enter into the analysis of the Coulomb dissociation experiments to extract the relevant capture cross section (see, e.g., the reviews in Refs. [12–14]). The nuclear contribution to the breakup should be small in comparison to the electromagnetic breakup. Fortunately, at the low binding energy of the proton in ^{8}B of 137 keV a large flux of equivalent photons is available so that nuclear excitation effects are comparatively small [15,16]. Also the kinematical conditions of the breakup reaction have an influence on the photon flux of different multipolarity. The E2 contribution, which is generally enhanced in the Coulomb dissociation as compared to the radiative capture reaction, has to be taken into account in the experimental analysis [17–19]. At higher energies, the observation of the resonant M1 breakup, suppressed at small projectiles energies, is a useful check of the method.

The Coulomb dissociation method also relies on the assumption that first-order perturbation theory is applicable. Therefore, deviations caused by higher-order effects have to be kept under control. The "post acceleration" of the fragments in the Coulomb field of the target after the breakup can lead to a distortion of the relative momentum distribution. There are various ways for a theoretical calculation of this effect. A fully quantum mechanical treatment is the post-form DWBA [20]. The most general methods in the semiclassical description of the excitation process are the coupled-channel approach [21–23] and the direct numerical integration of the time-dependent Schrödinger equation [24–28]. But these methods are rather involved numerically and only simple nuclear structure model Hamiltonians have been used up to now. For very fast excitations the sudden approximation may be used for the calculation of corrections to all orders in the electromagnetic interaction [29]. In Refs. [29,30] a method for the calculation of second-order corrections was developed in the approximation of small but finite adiabaticity parameters ξ. The virtue of this method is that it can be readily applied to different nuclear models. Intermediate states do not appear explicitly; instead, matrix elements of different effective operators have to be calculated between the initial and final states.

In this paper, it is the objective to improve our earlier calculation of the ^{8}B electromagnetic dissociation [30] in several aspects. We will extend the calculation of higher-order effects in the approximation of small adiabaticity parameters up to third-

order contributions. This enables us to get a better estimate for the range of validity of the small-ξ approximation. As the general method of the small-ξ approximation was explained in Refs. [29,30] we will only give a summary of the essential formulae in Section 2. We restrict ourselves to the straight-line approximation, appropriate to high-energy collisions, where the excitation functions can be expressed in terms of known functions.

The wave-like property of the projectile in the quantum mechanical description gives rise to diffraction effects which are absent in the semiclassical approximation. A simple method for the correction of the semiclassical excitation functions is developed in Section 3. This allows for a comparison of the significance of higher-order and nuclear effects. In Section 4 the nuclear model of the ^{8}B system is presented. In extension of the calculation in Ref. [30] also f-waves are included for the continuum states in the ^{7}Be-p motion. The results of the calculation are given in Section 5 for different kinematical conditions. We close in Section 6 with a summary and our conclusions.

2. Electromagnetic dissociation in perturbation theory

In the semiclassical approximation of the Coulomb excitation the relative motion of the projectile and the target is treated classically [31]. In medium- to high-energy heavy-ion collisions it is sufficient to assume a rectilinear motion of the projectile. Relativistic effects are included according to Ref. [32]. Corrections due to the Coulomb deflection of the projectile may be incorporated in a later stage of the calculation. We chose our coordinate system such that the projectile is at rest and the target moves with constant velocity v in the negative direction of the z-axis with $y = 0$ and $x = -b$. Assuming a pointlike target with charge number Z the time-dependent perturbation in the projectile system is given by

$$V(t) = \int \mathrm{d}^3 r \left[\rho(\boldsymbol{r}) \phi(\boldsymbol{r}, t) - \frac{1}{c} \boldsymbol{j}(\boldsymbol{r}) \cdot \boldsymbol{A}(\boldsymbol{r}, t) \right] \tag{1}$$

with the charge density $\rho(\boldsymbol{r})$ and the current density $\boldsymbol{j}(\boldsymbol{r})$ of the projectile. The scalar potential

$$\phi(\boldsymbol{r}, t) = \frac{Ze\gamma}{\left[(x+b)^2 + y^2 + \gamma^2 (z + vt)^2\right]^{1/2}} - \frac{Ze\gamma}{\left[b^2 + (\gamma v t)^2\right]^{1/2}} \tag{2}$$

and the vector potential

$$\boldsymbol{A}(\boldsymbol{r}, t) = -\frac{v}{c} \boldsymbol{e}_z \phi(\boldsymbol{r}, t) \tag{3}$$

are obtained from Ref. [32] by interchanging the role of the target and projectile as compared to the usual situation where the target at rest is excited. In time-dependent perturbation theory the excitation amplitude is expanded into a sum

$$a_{fi} = \delta_{fi} + a_{fi}^{(1)} + a_{fi}^{(2)} + a_{fi}^{(3)} + \ldots \tag{4}$$

of contributions of different order. From the excitation amplitude we obtain the triple differential cross section from

$$\frac{\mathrm{d}^3\sigma}{\mathrm{d}E\,\mathrm{d}\Omega_k\,\mathrm{d}\Omega_q}(J_i \to \boldsymbol{q}, S) = \frac{1}{2J_i+1}\sum_{M_i M_S}|a_{fi}|^2\frac{\mathrm{d}\sigma}{\mathrm{d}\Omega_k}\frac{\mu q}{(2\pi)^3\hbar^2} \tag{5}$$

for the excitation of the ground state $|i\rangle$ of the projectile with total angular momentum J_i to the final state $|f\rangle$ with channel spin S, relative momentum $\hbar\boldsymbol{q}$, and energy $E = \hbar^2 q^2/2\mu$ between the two fragments. The Rutherford cross section $\mathrm{d}\sigma/\mathrm{d}\Omega_k$ is calculated for the projectile c.m. scattering in the direction $\hbar\boldsymbol{k}$ depending on the impact parameter b. In general, the angular distribution of the fragments in the projectile c.m. system is a useful source of information for breakup contributions of different multipolarity through interference effects [33]. At high projectile energies and very forward angle scattering it will be difficult to extract the angular correlation from the experimental data with sufficient accuracy, unless special experimental methods are used. A possible way for the observation of interference effects is the measurement of momentum distributions of the fragments [4]. We will only give the double differential cross section which is obtained by an integration over the direction of $\hbar\boldsymbol{q}$.

2.1. First-order electromagnetic dissociation

The first-order contribution to the total amplitude is given by

$$a_{fi}^{(1)} = \frac{1}{\mathrm{i}\hbar}\langle f|V(\omega)|i\rangle \tag{6}$$

with

$$V(\omega) = \int_{-\infty}^{\infty}\mathrm{d}t\,\mathrm{e}^{\mathrm{i}\omega t}V(t) \tag{7}$$

and $\omega = (E_f - E_i)/\hbar = ck$. A multipole expansion of $V(\omega)$ leads to

$$V(\omega) = 4\pi Ze\sum_{\pi\lambda\mu}\frac{(-1)^\mu}{2\lambda+1}\mathcal{M}(\pi\lambda-\mu)S_{\pi\lambda\mu}(\xi) \tag{8}$$

with the usual electromagnetic multipole operators $\mathcal{M}(\pi\lambda\mu)$ for electric (π = E) and magnetic (π = M) transitions. We will use in the following the long-wavelength approximations:

$$\mathcal{M}(\mathrm{E}\lambda\mu) = \int \mathrm{d}^3r\,\rho(\boldsymbol{r})r^\lambda Y_{\lambda\mu}(\hat{r}) \tag{9}$$

and

$$\mathcal{M}(\mathrm{M}\lambda\mu) = \frac{-\mathrm{i}}{c(\lambda+1)}\int \mathrm{d}^3r\,\boldsymbol{j}\cdot\hat{\boldsymbol{L}}r^\lambda Y_{\lambda\mu}(\hat{r}). \tag{10}$$

The orbital integrals are given by

$$S_{\pi\lambda\mu}(\xi) = (-1)^{\lambda+1}\frac{(2\lambda+1)^{3/2}}{4\pi v\gamma}G_{\pi\lambda\mu}\left(\frac{c}{v}\right)k^{\lambda}K_{\mu}(\xi) \tag{11}$$

with modified Bessel functions $K_{\mu}(\xi)$ which depend on the adiabaticity parameter

$$\xi = \frac{\omega b}{v\gamma}. \tag{12}$$

The functions $G_{\pi\lambda\mu}$ can be expressed in terms of associated Legendre polynomials. They are defined in Ref. [32].

2.2. *Higher-order contributions for small adiabaticity parameters*

The second-order contribution in the small-ξ approximation are written here in a slightly different way as in [30]

$$a_{fi}^{(2)} = a_{fi}^{(2)}(\delta) + a_{fi}^{(2)}(\mathcal{P}). \tag{13}$$

They are decomposed into pole and principal value contributions

$$\begin{aligned} a_{fi}^{(2)}(\delta) = \frac{1}{2}\frac{1}{(\mathrm{i}\hbar)^2}\langle f|\Big\{ & V(\omega)V(\omega) + \xi V(\omega)\widetilde{V}(\omega) \\ & -\frac{b}{v\gamma\hbar}\left[V(\omega)H_0\widetilde{V}(\omega) - \widetilde{V}(\omega)H_0V(\omega)\right]\Big\}|i\rangle, \end{aligned} \tag{14}$$

$$\begin{aligned} a_{fi}^{(2)}(\mathcal{P}) = \frac{1}{(\mathrm{i}\hbar)^2}\frac{\mathrm{i}}{2\pi}\frac{b}{v\gamma\hbar}\mathcal{P}\int\frac{\mathrm{d}q}{q}\langle f|\Big\{ & V(\omega-q)V(\omega+q) \\ & +(E_f+E_i)V(\omega-q)\widetilde{V}(\omega+q) \\ & -V(\omega-q)H_0\widetilde{V}(\omega+q) - \widetilde{V}(\omega+q)H_0V(\omega-q)\Big\}|i\rangle, \end{aligned} \tag{15}$$

where we have defined

$$\widetilde{V}(\omega) = -\mathrm{i}\frac{v\gamma}{b}\int \mathrm{d}t\, t\mathrm{e}^{\mathrm{i}\omega t}V(t) = -\frac{v\gamma}{b}\frac{\mathrm{d}}{\mathrm{d}\omega}V(\omega). \tag{16}$$

H_0 is the Hamiltonian of the unperturbed projectile system. The product $V(\omega-q)V(\omega+q)$ is an even function of q and thus will give no contribution to the principal value integral. A multipole decomposition leads to

$$\widetilde{V}(\omega) = 4\pi Ze\sum_{\pi\lambda\mu}\frac{(-1)^{\mu}}{2\lambda+1}\mathcal{M}(\pi\lambda-\mu)R_{\pi\lambda\mu}(\xi) \tag{17}$$

with the functions

$$R_{\pi\lambda\mu}(\xi) = (-1)^{\lambda}\frac{(2\lambda+1)^{3/2}}{4\pi v\gamma}G_{\pi\lambda\mu}\left(\frac{c}{v}\right)k^{\lambda}\widetilde{K}_{\mu}^{\lambda}(\xi) \tag{18}$$

and

$$\widetilde{K}_{\mu}^{\lambda}(\xi) = \frac{1}{\xi^{\lambda}} \frac{\mathrm{d}}{\mathrm{d}\xi} \xi^{\lambda} K_{\mu}(\xi) = \frac{\lambda + \mu}{\xi} K_{\mu}(\xi) - K_{\mu+1}(\xi). \tag{19}$$

By angular momentum coupling we define the functions

$$T_{\lambda\mu}^{\pi_1\lambda_1\pi_2\lambda_2}(\xi_1, \xi_2) = \frac{2\lambda + 1}{(2\lambda_1 + 1)(2\lambda_2 + 1)} \times \sum_{\mu_1\mu_2} (\lambda_1 - \mu_1 \lambda_2 - \mu_2 | \lambda - \mu) S_{\pi_1\lambda_1\mu_1}(\xi_1) S_{\pi_2\lambda_2\mu_2}(\xi_2), \tag{20}$$

$$U_{\lambda\mu}^{\pi_1\lambda_1\pi_2\lambda_2}(\xi_1, \xi_2) = \frac{2\lambda + 1}{(2\lambda_1 + 1)(2\lambda_2 + 1)} \times \sum_{\mu_1\mu_2} (\lambda_1 - \mu_1 \lambda_2 - \mu_2 | \lambda - \mu) S_{\pi_1\lambda_1\mu_1}(\xi_1) R_{\pi_2\lambda_2\mu_2}(\xi_2) \tag{21}$$

and the operators

$$\mathcal{M}_2(\pi_1\lambda_1\pi_2\lambda_2\lambda - \mu) = \sum_{\mu_1\mu_2} (\lambda_1 - \mu_1 \lambda_2 - \mu_2 | \lambda - \mu) \times \mathcal{M}(\pi_1\lambda_1 - \mu_1) \mathcal{M}(\pi_2\lambda_2 - \mu_2), \tag{22}$$

$$\overline{\mathcal{M}}_2(\pi_1\lambda_1\pi_2\lambda_2\lambda - \mu) = \sum_{\mu_1\mu_2} (\lambda_1 - \mu_1 \lambda_2 - \mu_2 | \lambda - \mu) \times \mathcal{M}(\pi_1\lambda_1 - \mu_1) \overline{H}_0 \mathcal{M}(\pi_2\lambda_2 - \mu_2) \tag{23}$$

with

$$\overline{H}_0 = H_0 - \frac{E_i + E_f}{2}. \tag{24}$$

Here we have introduced slightly modified functions as compared to [30] in order to get a more convenient formulation of the amplitudes

$$a_{fi}^{(2)}(\delta) = \frac{1}{2} \left(4\pi \frac{Z_X e}{\mathrm{i}\hbar} \right)^2 \sum_{\lambda\mu} \frac{(-1)^{\mu}}{2\lambda + 1} \sum_{\pi_1\lambda_1\pi_2\lambda_2} \langle f | \mathcal{M}_2(\pi_1\lambda_1\pi_2\lambda_2\lambda - \mu) | i \rangle \times \left[T_{\lambda\mu}^{\pi_1\lambda_1\pi_2\lambda_2}(\xi, \xi) + \xi U_{\lambda\mu}^{\pi_1\lambda_1\pi_2\lambda_2}(\xi, \xi) \right] \tag{25}$$

$$a_{fi}^{(2)}(\mathcal{P}) = \frac{\mathrm{i}}{2\pi} \frac{-b}{v\gamma\hbar} \left(4\pi \frac{Ze}{\mathrm{i}\hbar} \right)^2 \sum_{\lambda\mu} \frac{(-1)^{\mu}}{2\lambda + 1} \sum_{\pi_1\lambda_1\pi_2\lambda_2} \langle f | \bar{\mathcal{M}}_2(\pi_1\lambda_1\pi_2\lambda_2\lambda - \mu) | i \rangle \times \mathcal{P} \int \frac{\mathrm{d}q}{q} \Big[U_{\lambda\mu}^{\pi_1\lambda_1\pi_2\lambda_2}(\xi - q, \xi + q) + (-1)^{\lambda_1 + \lambda_2 - \lambda} U_{\lambda\mu}^{\pi_2\lambda_2\pi_1\lambda_1}(\xi - q, \xi + q) \Big]. \tag{26}$$

In the limit $\xi \to 0$, corresponding to the sudden approximation, there will be no contribution from the principal value integral. Even in the case of finite ξ the contribution $a_{fi}^{(2)}(\mathcal{P})$ will vanish in certain cases. E.g. if higher-order contributions from only electric

multipolarities are considered and the potential in the Hamiltonian does not depend on the particle momenta, the matrix element $\langle f|\bar{\mathcal{M}}_2(\pi_1\lambda_1\pi_2\lambda_2\lambda-\mu)|i\rangle$ will vanish.

The contribution of third order $a_{fi}^{(3)}$ to the amplitude can be calculated in analogy to the second-order contribution in the low-ξ approximation. It can be decomposed into three contributions: a product term and two terms with a single and double principal value integral, respectively. The contribution of the single principal value integral vanishes again in the case $\xi \to 0$. The double principal value integral stays finite in this limit and assumes a value of $-\frac{1}{3}$ of the simple product term (cf. [31]). For finite but small adiabaticity parameters it will be sufficient in the following to neglect the contribution of the single principal value integral and to combine the remaining terms into the form

$$a_{fi}^{(3)} = \frac{1}{6}\frac{1}{(\mathrm{i}\hbar)^3}\langle f|V(\omega)V(\omega)V(\omega)|i\rangle. \tag{27}$$

In order to obtain a multipole decomposition we define the functions

$$\begin{aligned} V_{\bar{\lambda}\lambda\mu}^{\pi_1\lambda_1\pi_2\lambda_2\pi_3\lambda_3}(\xi_1,\xi_2,\xi_3) = {} & \frac{2\lambda+1}{(2\lambda_1+1)(2\lambda_2+1)(2\lambda_3+1)} \\ & \times \sum_{\substack{\mu_1\mu_2 \\ \mu_3\bar{\mu}}} (\lambda_1-\mu_1\lambda_2-\mu_2|\bar{\lambda}-\bar{\mu})(\bar{\lambda}-\bar{\mu}\lambda_3-\mu_3|\lambda-\mu) \\ & \times S_{\pi_1\lambda_1\mu_1}(\xi_1)S_{\pi_2\lambda_2\mu_2}(\xi_2)S_{\pi_3\lambda_3\mu_3}(\xi_3) \end{aligned} \tag{28}$$

and the operators

$$\begin{aligned} \mathcal{M}_3(\pi_1\lambda_1\pi_2\lambda_2\pi_3\lambda_3\bar{\lambda}\lambda-\mu) = {} & \sum_{\substack{\mu_1\mu_2 \\ \mu_3\bar{\mu}}} (\lambda_1-\mu_1\lambda_2-\mu_2|\bar{\lambda}-\bar{\mu})(\bar{\lambda}-\bar{\mu}\lambda_3-\mu_3|\lambda-\mu) \\ & \times \mathcal{M}(\pi_1\lambda_1-\mu_1)\mathcal{M}(\pi_2\lambda_2-\mu_2)\mathcal{M}(\pi_3\lambda_3-\mu_3). \end{aligned} \tag{29}$$

With these definitions we can write

$$\begin{aligned} a_{fi}^{(3)} = {} & \frac{1}{6}\left(4\pi\frac{Ze}{\mathrm{i}\hbar}\right)^3 \sum_{\lambda\mu}\frac{(-1)^\mu}{2\lambda+1} \sum_{\pi_1\lambda_1\pi_2\lambda_2\bar{\lambda}} \langle f|\mathcal{M}_3(\pi_1\lambda_1\pi_2\lambda_2\pi_3\lambda_3\bar{\lambda}\lambda-\mu) \\ & \times V_{\bar{\lambda}\lambda\mu}^{\pi_1\lambda_1\pi_2\lambda_2\pi_3\lambda_3}(\xi,\xi,\xi)|i\rangle. \end{aligned} \tag{30}$$

3. Diffraction effects

In the semiclassical approximation it is assumed that the projectile moves on a defined trajectory with a certain value of the impact parameter b corresponding to a specific scattering angle θ. The target is treated as a pointlike source of the electromagnetic field without any nuclear interaction. In fact, this is not the case. The target has a finite size and the strong interaction leads to a breakup or even absorption of the projectile when the mutual distance becomes too small. In a fully quantum mechanical calculation there

are contributions of trajectories with different impact parameters to a certain scattering angle and there are diffraction effects due to the wave-like nature of the projectile.

A comparison of the semiclassical approximation with a Glauber calculation of the breakup [34] leads to a simple correction of the semiclassical excitation functions to include diffraction effects. A more precise calculation of the diffraction effects including the nuclear contribution to the breakup will appear elsewhere [35]. Here, we will neglect the nuclear breakup but include diffraction effects in the eikonal approximation. In the semiclassical method the excitation amplitude depends on the impact parameter through the adiabaticity parameter in the functions $S_{\pi\lambda\mu}(\xi)$ (11). In the eikonal approximation of these functions an integral of the form

$$\int_0^\infty \mathrm{d}b'\, b' J_\mu(qb') K_\mu\left(\frac{\omega b'}{\gamma v}\right) \mathrm{e}^{\mathrm{i}\chi(b')} \tag{31}$$

is involved where the integration is carried out over all possible impact parameters b'. J_μ is a regular Bessel function,

$$q = 2k \sin\frac{\theta}{2} = \frac{2\eta}{b} \tag{32}$$

is the momentum transfer, and

$$\eta = \frac{Z_\mathrm{p} Z \mathrm{e}^2}{\hbar v} \tag{33}$$

is the Sommerfeld parameter for the projectile–target relative motion. The quantity

$$\chi(b') = -\frac{1}{\hbar v} \int_{-\infty}^{\infty} U_\mathrm{N}^\mathrm{opt}(z', b')\, \mathrm{d}z' + \psi_\mathrm{C}(b') \tag{34}$$

is the phase shift along a straight line with impact parameter b'. It consists of a contribution from the (optical) nuclear potential $U_\mathrm{N}^\mathrm{opt}$ of the target and the Coulomb contribution

$$\psi_\mathrm{C}(b') = 2\eta \ln\frac{\omega b'}{\gamma v}. \tag{35}$$

The divergence of the Coulomb phase for $b' \to 0$ is of no relevance in the following because the integrals involved converge nevertheless. We now replace everywhere the modified Bessel functions $K_\mu(\xi)$ in the definition of the Coulomb excitation functions by the eikonal expression

$$\mathcal{K}_\mu = \frac{q^2}{2\eta}(-\mathrm{i})^\mu \mathrm{e}^{-2\mathrm{i}\eta(\ln\xi - 1)} \int_0^\infty \mathrm{d}b'\, b' J_\mu(qb') K_\mu\left(\frac{\omega b'}{\gamma v}\right) \mathrm{e}^{\mathrm{i}\chi(b')}. \tag{36}$$

If the nuclear contribution to the phase $\chi(b')$ is neglected the approximation with the method of steepest descent leads to the result

$$\mathcal{K}_\mu^\mathrm{C} \approx K_\mu(\xi). \tag{37}$$

With the nuclear contribution we can write

$$\mathcal{K}_\mu = \mathcal{K}_\mu^{\mathrm{C}}(\xi) + \frac{q^2}{2\eta}(-\mathrm{i})^\mu \mathrm{e}^{-2\mathrm{i}\eta(\ln\xi - 1)} \int_0^\infty \mathrm{d}b'\, b' J_\mu(qb') K_\mu\left(\frac{\omega b'}{\gamma v}\right) \times \left[\mathrm{e}^{\mathrm{i}\chi(b')} - \mathrm{e}^{\mathrm{i}\psi_{\mathrm{C}}(b')}\right] \tag{38}$$

or approximately

$$\mathcal{K}_\mu \approx (1 + \mathcal{R}_\mu) K_\mu(\xi) \tag{39}$$

with the factor

$$\mathcal{R}_\mu = \frac{q^2}{2\eta}(-\mathrm{i})^\mu \mathrm{e}^{-2\mathrm{i}\eta(\ln\xi - 1)} K_\mu^{-1}(\xi) \int_0^\infty \mathrm{d}b'\, b' J_\mu(qb') K_\mu\left(\frac{\omega b'}{\gamma v}\right) \times \left[\mathrm{e}^{\mathrm{i}\chi(b')} - \mathrm{e}^{\mathrm{i}\psi_{\mathrm{C}}(b')}\right]. \tag{40}$$

Thus to correct for the diffraction effects we only have to multiply the semiclassical excitation functions $S_{\pi\lambda\mu}$ with the factor $(1 + \mathcal{R}_\mu)$. The total phase $\chi(b')$ depends on the specific shape of the nuclear potential, but for increasing b' it rapidly approaches the pure Coulomb phase so that there are no difficulties with the convergence of the integral. As a rough approximation we can assume that there is no nuclear contribution to the phase for impact parameters b' larger than the sum $b_{\min} = R_{\mathrm{p}} + R_{\mathrm{t}}$ of the projectile and target radii and that there is a complete absorption of the projectile for $b' < b_{\min}$. In this black disc approximation we have

$$\mathcal{R}_\mu = -\frac{q^2}{2\eta}(-\mathrm{i})^\mu \mathrm{e}^{-2\mathrm{i}\eta(\ln\xi - 1)} K_\mu^{-1}(\xi) \int_0^{b_{\min}} \mathrm{d}b'\, b' J_\mu(qb') K_\mu\left(\frac{\omega b'}{\gamma v}\right) \mathrm{e}^{\mathrm{i}\psi_{\mathrm{C}}(b')}. \tag{41}$$

The rapid oscillation of the Coulomb phase ψ_{C} causes no serious problems as the amplitude is damped in the integrand for decreasing b'.

4. Nuclear model of the ^{8}B system

Various approaches for the structure of the ^{8}B system can be found in the literature. They are either based on more or less simple potential models [26,36–42] or on more microscopic methods within cluster models [43–47] or on QRPA [5]. The nuclear system was also investigated in relation to the ^{7}Be(p,γ)^{8}B reaction by means of R-matrix theory [48] or from systematics within isobaric nuclei [49]. This is not the place for a full review of the different methods. On the whole, the models essentially agree on the energy dependence of the low-energy astrophysical S-factor. The main difference exists in the absolute value of the cross section, which is determined by the asymptotic normalization constant of the bound-state wave function [39]. But through

Table 1
Depths of the Woods–Saxon potential for various partial waves

l	0	1	1	1	2	3
J^π	2^-	1^+	2^+	3^+		
V_{lJ} [MeV]	56.180	43.556	46.570	35.400	50.000	50.000

the normalization of the bound state the absolute value of the asymptotic wave function is directly intertwined with the inner structure of the model wave function.

For the description of the ^{8}B system we essentially adopt our previous ^{7}Be-p single particle model [30] with small modifications as the inclusion of the f-wave in the scattering states and the treatment of the M1 resonance. The wave function of the relative motion of the proton and ^{7}Be which is taken to be structureless is obtained by solving the Schrödinger equation with the appropriate asymptotic conditions for bound and scattering states. The angular momentum $j = \frac{3}{2}$ of the ^{7}Be ground state is coupled with the spin $s = \frac{1}{2}$ of the proton to the channel spin $I = 2$. We neglect possible contributions of channel spin $I = 1$ in this approach. The potential in the Hamiltonian consists of a simple central Woods–Saxon potential

$$V(r) = -V_{lJ}\left[1 + \exp\left(\frac{r-R}{a}\right)\right]^{-1} \tag{42}$$

with a radius of $R = 2.39$ fm and a diffuseness parameter $a = 0.65$ fm. Depending on the total angular momentum J, the depth of the potential is adjusted in the p-waves to reproduce the binding energy $E_b = 0.137$ MeV of the ^{8}B ground state with $J^\pi = 2^+$ and the energies of the 1^+ resonance at 0.637 MeV and of the 3^+ resonance at 2.32 MeV [50]. Theses energies are given relative to the ^{7}Be-p breakup threshold. In this treatment it is not necessary to introduce an explicit spin–orbit potential as in Ref. [30]. In the other partial waves we adopt the potential depths of Ref. [36]. The precise values of V_{lJ} are given in Table 1. Additionally to our previous calculation we also consider f-waves for the scattering states. They become important for the E2 transitions at higher energies. The radial integration for the electromagnetic matrix elements is carried out up to a radius of 300 fm to achieve convergence at very small energies.

The M1 resonance at 0.637 MeV cannot be described sufficiently well in the simple single-particle model [30]. In order to estimate the effect of the M1 contribution to the breakup, we calculate M1 matrix elements independently from the above model for E1 and E2 matrix elements. Their energy dependence and amplitude was chosen to give the experimental width of (37 ± 5) keV [50] and a S-factor of 0.15 keV·b at the resonance energy which corresponds approximately to the experimental strength. The conclusions concerning the electromagnetic breakup will not be affected by this approximation. The M1 transition contributes only in the immediate vicinity of the resonance energy and there is no interference between first-order M1 and E1, E2 transitions.

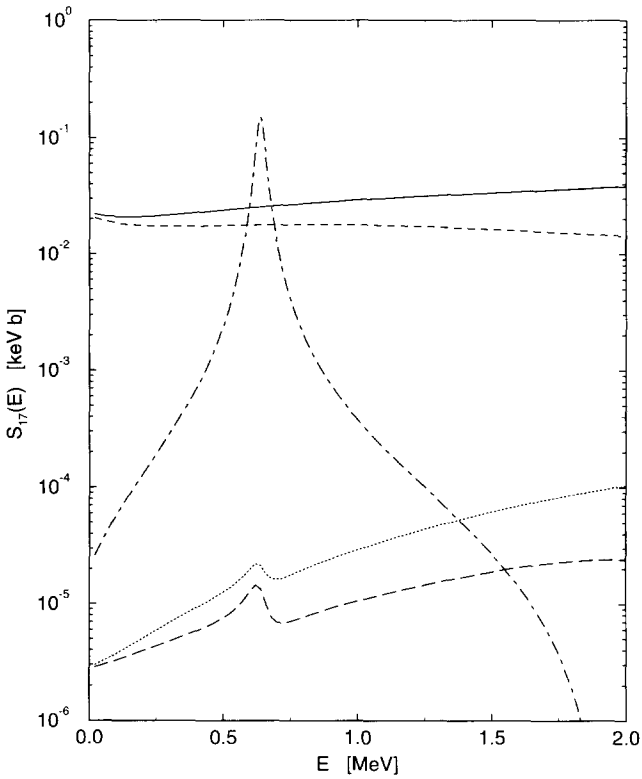

Fig. 1. Contributions to the astrophysical S-factor S_{17} of the ^{7}Be(p,γ)^{8}B reaction. E1: s-wave (dashed line), s- and d-wave (solid line); E2: p-wave (long-dashed line), p- and f-wave (dotted line); M1 (dot-dashed line).

5. Results

The contributions of the individual partial waves to the ^{7}Be(p,γ)^{8}B cross section, expressed as the astrophysical S-factor S_{17}, are shown in Fig. 1. The cross section is clearly dominated by E1 capture to the ground state from s- and d-waves except in the range of the M1 resonance. The E2 transitions give only a marginal contribution. The inclusion of the f-wave leads to a distinct increase of the E2 contribution at larger energies as compared to the earlier calculation [30]. This improvement of our calculation gives partial cross sections consistent with other single particle calculations [37,40] resolving former differences. From a summation of the contributions we obtain $S_{17}(20\ \text{keV}) = 22.08$ eV·b, a reasonable value compared to other calculations and the experimental results.

For an examination of the Coulomb dissociation cross section we will use the conditions of the experiments at RIKEN [8] with 46.5 A·MeV ^{8}B projectiles and the planned experiment at GSI with an energy of 250 A·MeV. For the first-order excitation

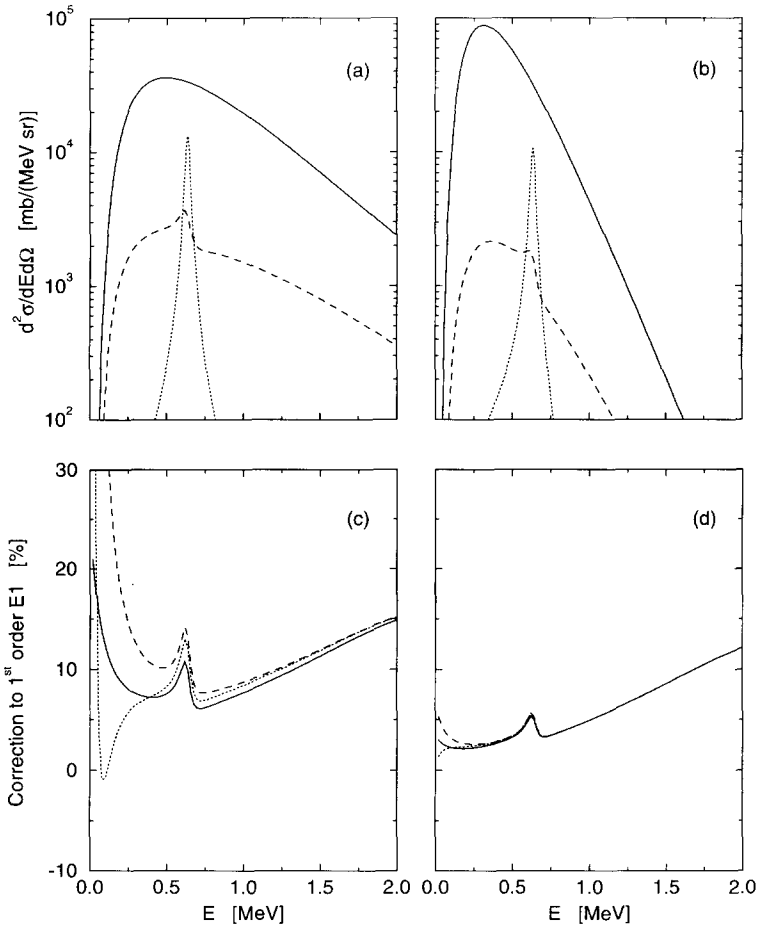

Fig. 2. Coulomb dissociation cross section of ^{8}B scattered on ^{208}Pb as a function of the relative energy for a projectile energy of 46.5 A·MeV and scattering angles of 1.5° (a+c) and 0.5° (b+d). Top panel (a+b): first-order results for E1 (solid line), E2 (dashed line), and M1 (dotted line). Bottom panel (c+d): corrections in % to the first-order E1 result; first-order E2 (solid line), first-order E2 + second-order (dashed line), first-order E2 + second- and third-order (dotted line).

contributions from E1, E2, and M1 transitions are considered. Second- and third-order corrections are calculated from all possible electric dipole and quadrupole couplings allowing transitions from the p-wave ground state to s-, p-, d-, and f-wave scattering states. There are no contributions from the principal value part in the second-order amplitude (26) in our model because we only consider electric excitations in the second- and third-order amplitudes. Higher-order effects from couplings with M1 are not taken into account as they will be important only near the resonance at 0.637 MeV.

To begin with, we study the dependence of the higher-order effects on the relative energy E between the fragments p and ^{7}Be for constant scattering angles typical for the experiments. In Fig. 2 the results for a projectile energy of 46.5 A·MeV are shown. The

dissociation cross section in first-order perturbation theory is given for two scattering angles in the top panel. The E1 contribution clearly dominates but the E2 contributions is considerably enhanced as compared to the capture reaction (cf. Fig. 1) due to the large flux of virtual quadrupole photons. The enhancement factor (E2 vs. E1) is approximately given by $4/(k_\gamma b)^2$ for small adiabaticity parameters. By way of contrast, the M1 contribution is strongly reduced at this projectile energy with a reduction factor of about $(v/c)^2$. Comparing the results for different scattering angles we notice the stronger decrease of the cross section with increasing relative energy for the smaller scattering angle. This is caused by the faster increase of the adiabaticity parameter at the larger impact parameters.

The main correction to the first-order E1 Coulomb dissociation cross section (bottom panel of Fig. 2) is the first-order E2 contribution, partly larger than 10%. For small relative energies corrections due to higher-order effects become important, especially for larger scattering angles, corresponding to small impact parameters. The second-order correction is always positive because the second-order amplitude is almost orthogonal to the first-order amplitude in our approach where we have no contribution from the principal value part. However, the third-order amplitude can interfere with the first-order amplitude leading to a reduction as compared to the first-order result. A similar observation ("dynamical quenching of E2") was made by the authors of Ref. [28] who calculated higher-order effects by a direct integration of the time-dependent Schrödinger equation: for very small impact parameters the breakup cross section was smaller than the simple sum of the first-order E1 and E2 contributions. Our perturbative calculation indicates a similar result but one may question the convergence of this method for very small impact parameters and relative energies. The strong increase of the higher-order corrections for $E \to 0$ is related to the behaviour of the E2/E1 ratio for decreasing $k_\gamma = (E + E_b)/\hbar c$. The pole in the expression for the ratio at the small binding energy of $E = E_b = 0.137$ MeV is almost reached. In the higher-order contributions the enhancement is more distinct due to multiple E2 excitations.

Results for a larger projectile energy of 250 A·MeV are shown in Fig. 3. Comparing the first-order results with the corresponding graphs for the smaller projectile energy (Fig. 2) we notice the increase of the M1 contribution, which should now be readily visible in the experiment, and tne reduction of the breakup caused by the E2 transitions. Second- and third-order effects are less significant, even at small relative energies.

The dependence of higher-order effects on the scattering angle for a fixed relative energy is a further point worth studying. This is done is Figs. 4 and 5 for the two projectile energies as above. We choose a relative energy of 0.3 MeV in the astrophysically interesting range. The breakup cross section is clearly dominated by first-order E1 excitation. The angular distribution is very forward peaked, especially at the higher projectile energies. The cross section drops rapidly for small scattering angles because the excitation becomes adiabatic. At large angles, corresponding to small impact parameters b, the E1 contribution decreases approximately with θ^{-2} whereas the E2 contribution stays almost constant. This different angular dependence in principle allows a separation of the multipole contribution in the analysis of experimental data [42]. But higher-order

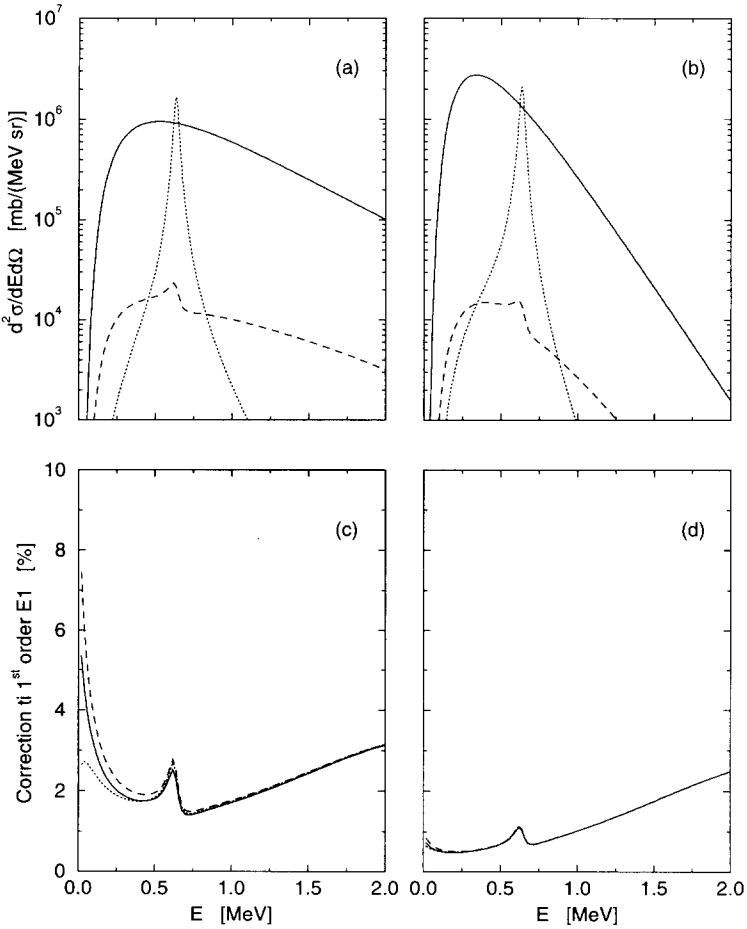

Fig. 3. Same as Fig. 2 but for a projectile energy of 250 A·MeV and scattering angles of 0.15° (left) and 0.05° (right).

effects and nuclear diffraction can spoil this simple relation limiting the possibility of extracting the E2 contribution from the experiment. Nevertheless, an attempt for the E2 extraction from the experimental data has been made taking into account nuclear-induced breakup in addition to Coulomb breakup [9].

As can be seen in the bottom part of Figs. 4 and 5 higher-order effects in the Coulomb excitation increase with the scattering angle for a projectile energy of 46.5 A·MeV. For too small impact parameters convergence of the perturbation series cannot be expected and other methods of calculation have to be considered. At higher projectile energies one does not have to worry about higher-order effects in the angular range where the breakup cross section is largest.

However, even larger than the higher-order effects in the electromagnetic interaction is the correction due to nuclear diffraction. It displays a typical angular dependence which

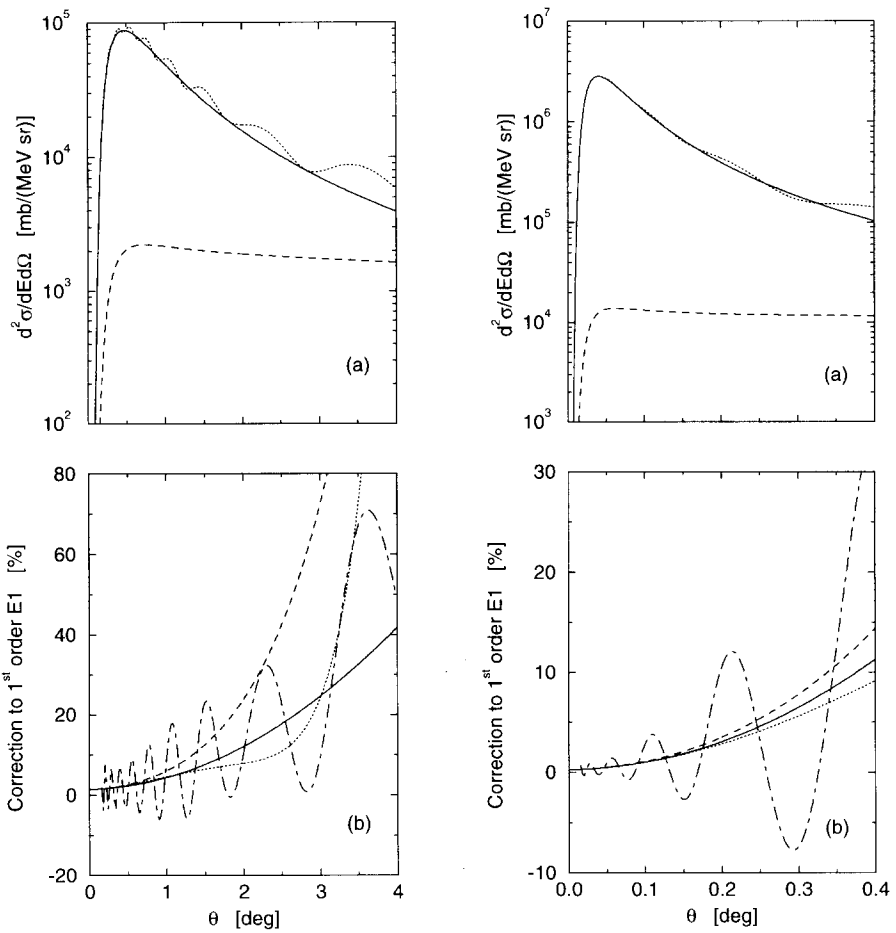

Fig. 4. Coulomb dissociation cross section of ^{8}B scattered on ^{208}Pb as a function of the scattering angle for a projectile energy of 46.5 A·MeV and a relative energy of 0.3 MeV. Top (a): first-order results for E1 (solid line) and E2 (dashed line), and E1+E2 including nuclear diffraction (dotted line). Bottom (b): corrections in % to the first-order E1 result; first-order E2 (solid line), first-order E2 + second-order (dashed line), first-order E2 + second- and third-order (dotted line), first-order E2 including nuclear diffraction (dot-dashed line).

Fig. 5. Same as Fig. 4 but for a projectile energy of 250 A·MeV.

is, of course, the black disc model used in our approach. But even a smoother transition into the absorptive region for small impact parameters will produce a noticeable effect. Angular integrated cross section will be much less sensitive to the diffraction effects. A further point worth studying is the contribution from nuclear-induced breakup [35,51] which will give a considerable contribution for large scattering angles where electromagnetic breakup ceases to dominate.

6. Summary and conclusions

We studied higher-order effects in the Coulomb dissociation of ^{8}B into ^{7}Be + p in high-energy scattering on a Pb target. This was achieved by a perturbation expansion of the excitation amplitude in orders of the electromagnetic interaction. We applied the semiclassical description of the excitation process for a straight-line motion of the projectile. Second- and third-order corrections were calculated in an approximation for small adiabaticity parameters which implicitly includes the summation over all intermediate states. This approach allows a simple estimate of the dependence of higher-order effects on the kinematical conditions of experiments. In principle, the method can be applied to different nuclear models for the projectile. We used a simple potential model for ^{8}B in our calculation. In general, the size of the higher-order effects may depend on the nuclear model used. A really model-independent extraction of the S-factor for the inverse ^{7}Be(p,γ)^{8}B reaction is only possible if first-order transitions dominate.

The inclusion of third-order corrections enabled us to examine the convergence of the perturbation approximation. At small impact parameters, low projectile and relative energies our approach becomes inadequate for the calculation of higher-order electromagnetic effects as can be expected. Then different methods have to be used. But under most experimental conditions considered so far the perturbation approach in the low-ξ approximation can serve as a reliable guide for the estimation of the higher-order corrections. At low projectile energies as in Ref. [52] our method is not appropriate.

First-order E1 excitation dominates clearly in the forward angle scattering. In the evaluation of the RIKEN experiments first-order E2 transitions have to be taken into consideration. However, higher-order effects play only a minor role in the range of relative energies measured until now. For energies below the M1 resonance higher-order effect may destroy the simple correspondence between Coulomb dissociation and radiative capture. At the high projectile energy of the proposed GSI experiment higher-order effects are well under control and a model-independent extraction of the E1 capture cross section should be possible even at rather small relative energies. Additionally, the absolute normalization of the cross section will benefit from the possible observation of the resonant M1 breakup. E2 contributions will be rather small and show up only at larger scattering angles where nuclear effects cannot be neglected.

Besides the electromagnetic dissociation we examined the effects of quantum mechanical diffraction caused by the absorption of the projectile in the nuclear field of the target. From the description of the breakup in Glauber theory a correction to the semiclassical approximation for the diffraction effect was obtained using the black disc approximation in order not to be dependent on the details of the nuclear interaction.

The diffraction produces the familiar oscillation of the cross section around the semiclassical prediction. The amplitude is often larger than the higher-order electromagnetic corrections. Even if higher-order effects are small it will be difficult to extract the E2 contribution from the angular dependence of the breakup cross section. Another problem, not considered in the present calculation, will be the nuclear-induced dissociation which also is important at large scattering angles. At present there are several efforts to

calculate the nuclear contribution to the breakup of ^{8}B [9,35,51].

Our calculation shows, that the E1 contribution, relevant to the capture reaction, can be reliably extracted in a model-independent way from the breakup, especially at the higher projectile energies. This will allow one to determine the absolute value of the low-energy S-factor independent of the direct measurements. The determination of the E2 component, however, is a difficult task [9,52] where the interpretation of experimental results needs the assistance of theoretical calculations.

Acknowledgements

This work was supported in part by the contract PAI P3-043 of the Belgian Office for Scientific Policy and by grant LMWolT from GSI.

References

[1] J.N. Bahcall, Neutrino Astrophysics (Cambridge Univ. Press, Cambridge, 1989).
[2] J.N. Bahcall and M.H. Pinsonneault, Rev. Mod. Phys. 67 (1995) 781.
[3] F.C. Barker and R.H. Spear, Astrophys. J. 307 (1986) 847.
[4] S. Typel, H.H. Wolter and H. Lenske, submitted to Phys. Lett. B.
[5] W. Schwab et al., Z. Phys. A 350 (1995) 283.
[6] I. Tanihata et al., Phys. Lett. B 206 (1988) 592.
[7] R.E. Warner et al., Phys. Rev. C 52 (1995) R1166.
[8] T. Motobayashi et al., Phys. Rev. Lett. 73 (1994) 2680.
[9] T. Motobayashi et al., Contribution to COSMOS'96, Notre Dame, U.S.A.
[10] T. Motobayashi et al., Phys. Lett. B 391 (1997) 261.
[11] S.E. Hirzebruch, private communication.
[12] G. Baur, C.A. Bertulani and H. Rebel, Nucl. Phys. A 458 (1986) 188.
[13] G. Baur and H. Rebel, J. Phys. G 20 (1994) 1.
[14] G. Baur and H. Rebel, Annu. Rev. Nucl. Part. Sci., to be published.
[15] C.A. Bertulani, Phys. Rev. C 49 (1994) 2688.
[16] R. Shyam, I.J. Thompson and A.K. Dutt-Mazumder, Phys. Lett. B 371 (1996) 1.
[17] K. Langanke and T.D. Shoppa, Phys. Rev. C 49 (1994) R1771; 51 (1995) 2844.
[18] M. Gai and C.A. Bertulani, Phys. Rev. C 52 (1995) 1706.
[19] K. Langanke and T.D. Shoppa, Phys. Rev. C 52 (1995) 1709.
[20] R. Shyam, P. Banerjee and G. Baur, Nucl. Phys. A 540 (1992) 341.
[21] C.A. Bertulani and F. Canto, Nucl. Phys. A 539 (1992) 163.
[22] L.F. Canto, R. Donangelo, A. Romanelli and H. Schulz, Phys. Lett. B 318 (1993) 415.
[23] C.A. Bertulani, GSI-preprint 05-96 (1996).
[24] C.A. Bertulani and G.F. Bertsch, Nucl. Phys. A 556 (1993) 136; Phys. Rev. C 49 (1994) 2839.
[25] T. Kido, K. Yabana and Y. Suzuki, Phys. Rev. C 50 (1994) R1276.
[26] H. Esbensen, G.F. Bertsch and C.A. Bertulani, Nucl. Phys. A 581 (1995) 107.
[27] C.A. Bertulani, Nucl. Phys. A 587 (1995) 318.
[28] H. Esbensen and G.F. Bertsch, to be published.
[29] S. Typel and G. Baur, Nucl. Phys. A 573 (1994) 486.
[30] S. Typel and G. Baur, Phys. Rev. C 50 (1994) 2104.
[31] K. Alder and A. Winther, Electromagnetic Excitation (North-Holland, Amsterdam, 1975).
[32] A. Winther und K. Alder, Nucl. Phys. A 319 (1979) 518.
[33] G. Baur and M. Weber, Nucl. Phys. A 505 (1989) 448.
[34] C.A. Bertulani und A.M. Nathan, Nucl. Phys. A 554 (1993) 158.
[35] A. Mündel and G. Baur, Nucl. Phys. A 609 (1996) 254.

[36] F.C. Barker, Aust. J. Phys. 33 (1980) 177.
[37] K.H. Kim, M.H. Park and B.T. Kim, Phys. Rev. C 35 (1987) 363.
[38] F.C. Barker, Phys. Rev. C 37 (1988) 2920.
[39] A.M. Mukhamedzhanov and N.K. Timofeyuk, JETP Lett. 51 (1990) 282; Sov. J. Nucl. Phys. 51 (1990) 431.
[40] H. Krauss, K. Grün, T. Rauscher and H. Oberhummer, Ann. Phys. 2 (1993) 320.
[41] K. Riisager and A.S. Jensen, Phys. Lett. B 301 (1993) 6.
[42] H. Esbensen and G.F. Bertsch, Phys. Lett. B 359 (1995) 13; Nucl. Phys A 600 (1996) 37.
[43] E. Kolbe, K. Langanke and H.J. Assenbaum, Phys. Lett. B 214 (1988) 169.
[44] P. Descouvement and D. Baye, Nucl. Phys. A 487 (1988) 420.
[45] C.W. Johnson, E. Kolbe, S.E. Koonin and K.H. Langanke, Astrophys. J. 392 (1992) 320.
[46] P. Descouvement and D. Baye, Nucl. Phys. A 567 (1994) 341.
[47] A. Csótó, K. Langanke, S.E. Koonin and T.D. Shoppa, Phys. Rev. C 52 (1995) 1130.
[48] F.C. Barker, Nucl. Phys. A 588 (1995) 693.
[49] B.A. Brown, A. Csótó and R. Sherr, Nucl. Phys. A 597 (1996) 66.
[50] F. Ajzenberg-Selove, Nucl. Phys. A 490 (1988) 1.
[51] K. Hencken, G. Bertsch and H. Esbensen, Preprint DOE/ER/40561-271-INT96-00-132.
[52] J. von Schwarzenberg et al., Phys. Rev. C 53 (1996) R2598.